



Digging into the roots of belowground carbon cycling following seven years of Prairie Heating and CO₂ Enrichment (PHACE), Wyoming USA



Laura Nelson ^a, Dana M. Blumenthal ^b, David G. Williams ^a, Elise Pendall ^{a, c, *}

^a Department of Botany, University of Wyoming, 1000 East University Avenue, Laramie, WY 82071, USA

^b Rangeland Resources Research Units, USDA-ARS, Crops Research Laboratory, 1701 Centre Avenue, Fort Collins, CO 80526, USA

^c Hawkesbury Institute for the Environment, University of Western Sydney, Penrith, 2751 NSW, Australia

ARTICLE INFO

Article history:

Received 1 March 2017

Received in revised form

13 August 2017

Accepted 22 August 2017

Available online 4 September 2017

Keywords:

Elevated CO₂

Warming

Fine-roots

Priming

Carbon cycling

ABSTRACT

Grassland soils are significant carbon (C) sinks as more than half of grassland plant biomass is belowground and roots are the main source of soil C. It is uncertain if grassland soils will continue as C sinks in the future because climate change may affect the dynamic, belowground relationships among crown and root biomass, root chemistry and morphology, and root and soil decomposition, all of which influence C sequestration potential. To better understand future belowground C cycling in semiarid grasslands we analyzed three native species (*Bouteloua gracilis*, *Carex eleocharis*, and *Pascopyrum smithii*) and mixed-grass community crown and root biomass, root chemistry, morphology, and decomposability, and soil organic carbon (SOC) priming following seven years of simulated climate change at the Prairie Heating and CO₂ Enrichment (PHACE) experiment in Wyoming, USA. We found that individual species and the community respond uniquely to the climate change field treatments, indicating that species composition is important when analyzing climate change effects on grassland C cycling. Root biomass in the C3 sedge, *C. eleocharis*, increased under elevated CO₂, especially when combined with warming. Decomposition rates of roots from warming plots were higher than those from ambient plots for *B. gracilis* and *P. smithii*. Across species, root decomposition rates increased with C and N concentrations. Root morphology was altered as well: *B. gracilis* root diameter increased under warming, and *P. smithii* specific root length and surface area increased under elevated CO₂. *P. smithii* roots induced short-term, negative SOC priming across all field treatments. Together, our results indicate that grass roots may play a critical role in maintaining soil C stocks in grasslands in the future.

© 2017 Elsevier Ltd. All rights reserved.

1. Introduction

Grasslands contain more than 10% of the global carbon (C) stock and 98% of that C is in the soil (Jones and Donnelly, 2004; Heinemeyer et al., 2012). The significant amount of C in grassland soils may be attributed to the high root:shoot ratios that characterize grasslands (Mokany et al., 2006). For example, 90% of plant biomass and 67% of NPP in semiarid shortgrass steppe is concentrated belowground (LeCain et al., 2006). Additionally, temperate grasslands contain 17% of the global fine-root pool (less than 2-mm diameter) (Jackson et al., 1997). A large portion of belowground C is also stored as carbohydrates in crowns just below the soil surface

(Milchunas and Lauenroth, 2001). The large quantity of C stored belowground in grasslands makes relationships among biomass, fine-root chemistry, morphology, and decomposition critical, because as CO₂ concentrations and temperatures rise, the dynamics of these components and their impacts on grassland C cycling may change (Silver and Miya, 2001; Hui and Jackson, 2006; de Graaff et al., 2011; White et al., 2012).

Biomass accumulation and plant tissue quality often influence one another, thus changes in biomass in response to climate change may be reflected in root chemistry (Craine et al., 2003). Increases in belowground biomass, root C:N, and longevity often co-occur under elevated CO₂ (van Groenigen et al., 2005; Dijkstra et al., 2010; Pendall et al., 2011; Dieleman et al., 2012). This contrasts with warming treatments, where fine-root biomass decreases or does not significantly change, root C:N generally decreases, and N mineralization increases (Pendall et al., 2011; Dieleman et al., 2012; Carrillo et al., 2014). In an Australian native grassland, elevated CO₂

* Corresponding author. Department of Botany, University of Wyoming, 1000 East University Avenue, Laramie, WY 82071, USA.

E-mail address: e.pendall@westernsydney.edu.au (E. Pendall).

paired with warming increased root biomass, but root C:N responses were dependent on plant functional type and N distribution (Pendall et al., 2011). Therefore, assessing root biomass and chemistry responses to climate change by species may reveal important insights into belowground sources and sinks of carbon.

Known controls over fine-root decomposition include root quality, root morphology, microbial composition, and environment (Silver and Miya, 2001; Vivanco and Austin, 2006; Birouste et al., 2012; Pilon et al., 2013; Bardgett et al., 2014; Smith et al., 2014). Root decomposition may decrease with elevated CO₂ due to an increase in root C:N and/or lignin and suberin concentrations (Gorissen et al., 1995; van Groenigen et al., 2005; de Graaff et al., 2011; Pendall et al., 2011). Also under elevated CO₂, N-limitation tends to favor roots with large diameters, low specific root lengths (SRL, length per unit mass), and greater root-tissue densities (RTD, mass per volume) (Dieleman et al., 2012). Roots with these characteristics tend to have long lifespans (Bardgett et al., 2014; Reich and Cornelissen, 2014; Prieto et al., 2015). In contrast to elevated CO₂ effects, warming may lower C:N ratios, resulting in accelerated root decomposition (Silver and Miya, 2001; Pendall et al., 2004). The increase in N-availability with warming also appears to favor roots with small diameters, high SRLs, small RTDs, and short lifespans (Dieleman et al., 2012). However, in water-limited ecosystems, where elevated CO₂ increases water content and warming induces soil desiccation (Nowak et al., 2004; Morgan et al., 2011), water-mediated effects might counter N-mediated effects (Dieleman et al., 2012; Pilon et al., 2013; Reich and Cornelissen, 2014). For example, in low moisture ecosystems, root decomposition appears to be accelerated under elevated CO₂ (Allard et al., 2005; Dijkstra et al., 2008; Carrillo et al., 2014). Since both root decomposition and root morphology appear to be impacted by elevated CO₂ and warming, and root morphology appears to influence root lifespan, quantifying both root-morphological traits and root decomposition rates in response to climate change may provide a key link in understanding C transfer from roots to the soil (Eissenstat et al., 2000).

Fine-roots are quite labile relative to SOC and may induce a positive or negative priming effect on SOC decomposition (Mary et al., 1992; de Graaff et al., 2013). Positive priming is an increase, while negative priming is a decrease, in the amount or rate of SOC decomposition (Kuzyakov et al., 2000). Past studies show changes in the amount, quality, and morphology of fine-roots in response to elevated CO₂ or warming (van Groenigen et al., 2005; Morgan et al., 2011; Pendall et al., 2011; Dieleman et al., 2012; Carrillo et al., 2014). Therefore, the effects of increased temperature and atmospheric CO₂ on root dynamics and properties may impact the direction and extent of root-induced priming of SOC, ultimately affecting C storage in grassland soils.

Climate change factors are expected to interactively alter species composition in native plant communities, depending on the resistance or vulnerability of individual species (Zelikova et al., 2014). After prolonged exposure to elevated CO₂ and warming at the Prairie Heating and CO₂ Enrichment (PHACE) experiment, grassland community composition shifted to favor subdominant, C3 species (especially the drought-tolerant sedge, *Carex eleocharis*), at the expense of the dominant C4 species (*Bouteloua gracilis*) (Zelikova et al., 2014; Mueller et al., 2016). We expected that these species shifts could be associated with changes in belowground resource availability, different root traits, and altered soil C cycling. Indeed, elevated CO₂ combined with warming led to lower soil moisture and higher soil inorganic N in comparison with the control treatment (Mueller et al., 2016; Carrillo et al., 2012), larger root biomass and longer, thinner roots at the community-level (Mueller et al., 2016; Carrillo et al., 2014), and enhanced rates of SOC decomposition (Pendall et al., 2013). However, until the end of the

PHACE experiment in 2013 no species-level sampling was conducted belowground.

The objective of this study was to better understand future belowground C cycling in semiarid grasslands by analyzing linkages between climate change effects on belowground biomass with fine-root chemistry, morphology, and decomposition, and SOC priming, particularly at the species-level. We predicted that 1) crown biomass responses to climate change treatments would be similar to root biomass responses for all species; 2) root chemical (C and N concentrations) and morphological responses to climate change treatments would depend on species identity; 3) root decomposition rates and priming of SOC decomposition would be related to root C and N contents and morphology (diameter, specific root length and surface area). We thus expected that intrinsic differences in root traits between native grassland species would mediate soil C cycle responses to climate change (Pendall et al., 2011; Burke et al., 2013).

2. Materials and methods

2.1. Study site

This experiment was conducted at the Prairie Heating and CO₂ Enrichment (PHACE) experiment located at the USDA-ARS High Plains Grassland Research Station (HGRS), 15 km west of Cheyenne, WY (41° 11' N, 104° 54' W; elevation 1930 m) (Carrillo et al., 2011). The PHACE site vegetation is classified as a northern mixed grass prairie composed of grasses and forbs, including a C₃ grass species *Pascopyrum smithii* (Rydb.) A. Love and a C₄ grass species *Bouteloua gracilis* (H.B.K.) Lag., which together comprise 50% of the total aboveground biomass, and a sedge, *Carex eleocharis* L. Bailey (Dijkstra et al., 2010). Annual precipitation averaged 384 mm and average air temperature was −2.5 °C in winter and 17.5 °C in summer (Morgan et al., 2011; Carrillo et al., 2014). The soil was an Ascalon variant loam on the north side of the field site and an Altvan loam on the south side of the field site (Dijkstra et al., 2010; Nie et al., 2013).

2.2. Field experiment

The PHACE experiment included twenty, 3.4 m diameter circular plots divided into four combinations of elevated CO₂ and warming, with five replicates of each combination (Dijkstra et al., 2010; Carrillo et al., 2011). The four field treatments included ambient CO₂ and ambient temperature (ct), ambient CO₂ and elevated temperature (cT), elevated CO₂ and ambient temperature (Ct), and elevated CO₂ and elevated temperature (CT). The ambient [CO₂] was approximately 400 μmol mol^{−1} and the elevated [CO₂] was 600 ± 40 μmol mol^{−1} (Morgan et al., 2011). The elevated temperatures were 1.5 °C above ambient during the day and 3.0 °C above ambient at night (LeCain et al., 2015). Free air CO₂ enrichment (FACE) was implemented during the growing season beginning in April 2006; temperatures were elevated year-round with infrared heaters attached 1.5 m above the ground on frames starting in March 2007 (Morgan et al., 2011; LeCain et al., 2015). The experiment was terminated in mid-July 2013, when all samples for this work were harvested.

2.3. Field sampling

We collected soil samples from 0 to 5 cm depth by compositing four, 5 cm diameter cores from each of the twenty field plots. The soil was sieved with 2 mm sieves, weighed on site, and then transported back to the lab in coolers. We removed roots and aboveground litter by hand-picking the soil samples and then

stored them at 2 °C for nine days.

Crown and root biomass of *B. gracilis*, *C. eleocharis*, and *P. smithii* were collected from each of the twenty treatment plots by excavating blocks of soil 10-cm deep and 25 by 25 cm area from each treatment plot and transporting the soil blocks to the laboratory in coolers. *B. gracilis*, *C. eleocharis*, and *P. smithii* roots were separated from each block by identifying the grass species in each block aboveground, tracing the plant through the soil block down to its crowns and roots, and then clipping the stems and roots from the crowns. We recovered on average 80% of the total crown biomass and 42% of the total root biomass in the three species studied (Supplemental Table 1). This is similar to the method used in a nearby prairie, where about 33% of roots were identifiable to species to a depth of 75 cm (LeCain et al., 2006), but we did not use hair detangler. Community-level roots and crowns, not distinguished by species, were collected in a similar way from another set of 25 by 25 cm blocks.

2.4. Biomass and root chemistry

Crown and root samples were washed in deionized water for 30 min on a shaker bench and then dried at 70 °C for ten days prior to weighing. The root biomass values represent minimum amounts due to breakage of roots during collection, and the 10-cm depth of harvest. Subsamples of clean, dry crowns and roots were ground in a ball mill and ashed at 550 °C for 3 h, and % C \pm SD 0.2, % N \pm SD 0.04, and C:N were measured on a Costech 4010 Elemental Analyzer (Costech Analytical Technologies Inc., Valencia, CA, United States of America).

2.5. Root morphology

Subsets of *B. gracilis*, *C. eleocharis*, *P. smithii*, and community roots from each field treatment plot were analyzed with WinRhizo Pro 2009 software (Regent Instruments Inc., Quebec, Canada). Approximately 150 mg of fresh roots were weighed, washed with DI water, and hand-placed using tweezers to minimize overlap. A clear transparency was placed on top of roots prior to scanning with an Epson Perfection 4870 scanner (Epson, Long Beach, CA, United States of America). After scanning, roots were oven-dried at 55 °C and re-weighed.

In WinRhizo all scanned-root images were analyzed at 800 DPI using a color analysis with three groups, two color classes each, to differentiate blue-sheet background color from roots. Prior to analyzing scanned-root images, any non-root debris was hand-selected on the digitized image and excluded. Following analysis, each image was inspected for error, including but not limited to, incomplete tracing of roots and root hairs and analysis of non-root components. Root parameters selected from the image analysis included total root length (mm), average root diameter (mm), total root surface area (mm²), and total root volume (mm³). From these parameters diameter (mm), RTD (mg mm⁻³), SRL (mm mg⁻¹), and SRSA (mm² mg⁻¹), were calculated on a dry weight basis.

2.6. Laboratory incubation setup and sampling

To quantify potential decomposition, we incubated *P. smithii*, *B. gracilis*, and community roots in sand (Roots + Sand). For each species, we added 75 mg of clean, dry roots cut into 1 cm-lengths to 15 g of muffled sand (3 h, 550 °C) and 1 ml of soil slurry. The slurry consisted of 120 g of fresh soil collected from the field site at 0–5 cm depth, sieved to 2 mm, and combined with 100 ml DI water. We added soil slurry to confirm microbial activity since the roots were dried to stop autotrophic respiration; slurry controls contained 1 ml of soil slurry in 15 g of muffled sand. To quantify soil C

decomposition and priming by root C, we incubated soil (Soil) and soil with *P. smithii* roots (Soil + Roots). For Soil, we weighed 15 g of soil into 50 ml plastic beakers, with each beaker containing soil sampled from one of the twenty field plots. For Soil + Roots, we added 75 mg of dried 1 cm-cut *P. smithii* roots to 15 g of soil, combining roots and soil from the same field plot.

We began the incubation by bringing water content to 60% of field capacity, compressing the mixture to simulate *in situ* bulk density, and then weighing and placing each beaker into a clean 500 ml glass-canning jar. All jars were sealed tightly and stored in the dark. The Soil and Soil + Roots jars were stored at approximately 18.5 °C and the root plus sand jars at approximately 20 °C. Six jars containing only an empty beaker were used as controls.

Headspace CO₂ concentrations were determined on a LI-820 gas analyzer (Li-Cor 820, LICOR Inc., Lincoln, NE, United States of America) coupled to a Valco 6-port valve and 2-ml sampling loop. After sampling, jars were opened and vented outside with a small hand-held fan. We measured the $\delta^{13}\text{C}$ values of headspace CO₂ in order to partition root and soil C contributions. For isotope sampling, 15 ml samples were injected into evacuated Exetainer vials and analyzed on a Thermo Gasbench coupled to a Thermo Delta Plus XL IRMS (ThermoScientific Bremen, Germany). Analytical precision was \pm SD 0.1‰ for $\delta^{13}\text{C}$. We sampled the Soil and Soil + Roots jars for CO₂ on days 1, 3, 5, 8, 12, 19, 29, 35, 42, 50, 63, 79, and 94, for isotopes on days 3, 12, 29, and 50, 63, and 94, and adjusted water content on days 13, 32, 57, and 75. We sampled the root plus sand jars for CO₂ on days 1, 3, 6, 8, 12, 22, 30, 36, 43, and 58, for isotopes on days 3 and 12, and adjusted water content on days 13 and 34.

2.7. Data analysis

To assess the dynamics of the labile and resistant root C pools, a two-pool, three-parameter, exponential decay model was applied to CO₂ production rates over time (after blank correction) using nonlinear curve fitting in Sigma Plot 13.0 (Eq. (1)) (Carrillo et al., 2011).

$$R_t = R_l \times e^{K_l t} + R_r \quad (1)$$

where R_t = rate of CO₂ production at time t ($\mu\text{g C g root d}^{-1}$), R_l = labile root C decomposition rate, R_r = resistant root C decomposition rate and K_l = intrinsic decay constant of root C in the labile pool (d^{-1}).

We used a two-part isotope mixing model to quantify the fraction of SOC-derived CO₂ in Soil + Roots jars for each sampling date, after correcting for blank CO₂ concentrations and $\delta^{13}\text{C}$ values (Pendall and King, 2007) (Eq. (2))

$$f_{\text{SOC-CO}_2} = \left(\frac{\delta^{13}\text{C}_{\text{SR}} - \delta^{13}\text{C}_{\text{R}}}{\delta^{13}\text{C}_{\text{S}} - \delta^{13}\text{C}_{\text{R}}} \right) \quad (2)$$

where $f_{\text{SOC-CO}_2}$ = fraction of SOC-derived CO₂, $\delta^{13}\text{C}_{\text{SR}}$ = $\delta^{13}\text{C}$ Soil + Roots, $\delta^{13}\text{C}_{\text{R}}$ = $\delta^{13}\text{C}$ *P. smithii* roots plus sand, $\delta^{13}\text{C}_{\text{S}}$ = $\delta^{13}\text{C}$ Soil. We quantified priming as the difference in SOC-derived CO₂ flux rate with and without roots (Eq. (3))

$$R_{\text{primedSOC}} = (f_{\text{SOC-CO}_2} \times R_{\text{SR}}) - (R_{\text{S}}) \quad (3)$$

where $R_{\text{primedSOC}}$ = rate of primed C ($\text{mg C g soil}^{-1} \text{ day}^{-1}$), R_{SR} = decomposition rate of Soil + Roots ($\text{mg C g soil}^{-1} \text{ day}^{-1}$), and R_{S} = decomposition rate of Soil ($\text{mg C g soil}^{-1} \text{ day}^{-1}$). We then determined cumulative SOC decomposition with and without roots over the 94-day incubation period.

2.8. Statistics

A two-factor factorial (CO₂ by temperature) mixed-model, with a random block term for soil type, was used to analyze biomass, root chemistry, root morphology, and root decomposition parameters for each species and the community. *Post hoc* testing was performed with least square means separation with Tukey-Kramer adjustment. Pearson correlation matrices and simple linear regression were used to determine relationships between biomass, root chemistry, morphology, and decomposition traits by species and the community. Data that did not meet assumptions of equal variances following Hartley's method or normality of residuals were log, square root, or quarter power-transformed. When transformations did not equalize variances, a weighted analysis was performed (Eq. (4)).

$$\text{Weights} = \frac{1}{\sqrt{S_{ij}^2}} \quad (4)$$

where S_{ij}^2 were the variances of the *i*th level of CO₂ by warming combination and *j*th level of root ID. Influential data points in linear regression analyses, points that met all of three requirements, studentized residuals >2, leverages >0.5, and Cook's D > 4 (n-k-1)⁻¹, were analyzed in linear regression plots; points were then removed if removal resulted in change in significance and/or direction of slope. No data points were removed.

A repeated measure analysis for a two-way analysis of variance (ANOVA), CO₂ by temperature, with a blocking term for soil type, was used to examine the priming results. When sphericity failed, the adjusted Huynh-Feldt-Lecoutre Epsilon (H-F-L) results were used. We used a three-way ANOVA (CO₂ by temperature by incubation treatment), split-plot completely randomized design to statistically compare treatment effects on cumulative SOC decomposition. Least square means separation with Tukey-Kramer adjustment was used for *Post hoc* analyses. All statistical analyses were performed with α of 0.05 in SAS v. 9.4 (SAS Institute Inc., Cary, NC, United States of America). Significant statistical results are presented clearly in figures and tables in order to streamline the text.

3. Results

3.1. Biomass

Elevated CO₂ and warming interacted to alter crown biomass of *B. gracilis* and *C. eleocharis*, but in opposite directions (Fig. 1a). While *B. gracilis* crowns expanded with warming alone, *C. eleocharis* crowns decreased with warming but only at ambient CO₂ (Fig. 1a). By contrast, *P. smithii* crown biomass showed no significant differences (Fig. 1a). Likewise, crowns from the community harvest showed no treatment effects ($P > 0.05$; mean = 260 ± 44.2 g m⁻²).

Root biomass was not significantly affected by warming or elevated CO₂ in *B. gracilis* or *P. smithii* (Fig. 1b). In contrast, *C. eleocharis* root biomass increased with the main effect of elevated CO₂ by 171% from ambient CO₂ levels (Fig. 1b). Community level root biomass averaged 216 ± 55.2 g m⁻² across the treatments ($P > 0.05$).

3.2. Root chemistry

Warming and elevated CO₂ affected individual species and community root C, N, and C:N ratios in different ways (Table 1). There was a significant interaction between warming and CO₂ for

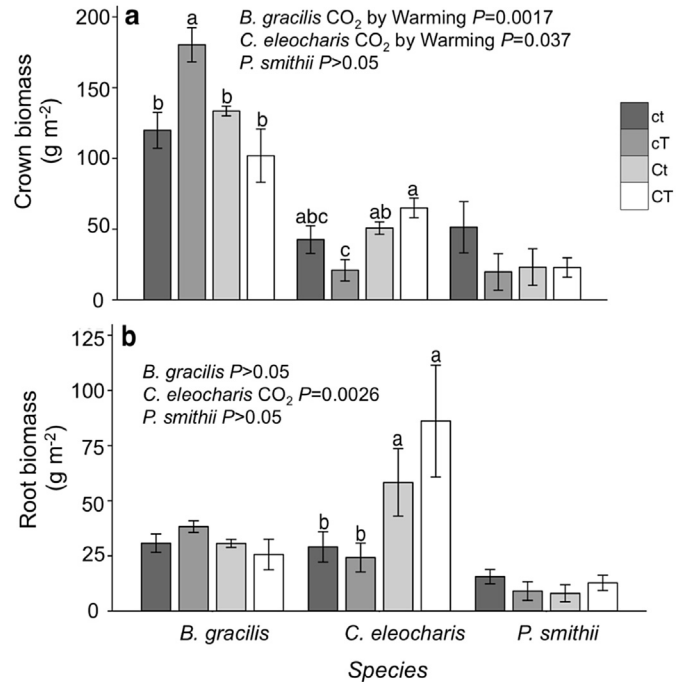


Fig. 1. Average belowground biomass of *B. gracilis*, *C. eleocharis*, and *P. smithii* in a) crowns and b) roots from 0–10 cm depth after seven years of elevated CO₂ and warming grouped into four field treatments: ct = ambient CO₂ and temperature, cT = ambient CO₂ and elevated temperature, Ct = elevated CO₂ and ambient temperature, and CT = elevated CO₂ and temperature. Values are means ± standard error; P-values are from two-way ANOVA, CO₂ by temperature, and letters show means separations (Tukey-Kramer adjustment).

B. gracilis root C, with a positive effect in the combined treatment (Table 1). A warming and CO₂ interaction significantly affected *P. smithii* root C, with an increase of 43% in the elevated CO₂ treatment compared to ambient (Table 1). Both *C. eleocharis* and community root C were not statistically different among the four field treatments ($P > 0.05$).

Both *B. gracilis* and *P. smithii* root N responded to the main effect of CO₂ (Table 1). *B. gracilis* root N decreased by an average 14% whereas *P. smithii* root N increased by an average 8% compared to ambient CO₂. Also, community root N increased under the main effect of warming by 21%. The climate change field treatments did not significantly affect root N of *C. eleocharis* ($P > 0.05$).

C. eleocharis and community root C:N were altered by either elevated CO₂ or warming (Table 1). *C. eleocharis* root C:N increased under the main effect of elevated CO₂, while community root C:N decreased under the main effect of warming. There was no significant change in root C:N for *B. gracilis* or *P. smithii* across the four field treatments ($P > 0.05$).

3.3. Root morphology

Three of the four analyzed root morphological traits, diameter, SRL, and SRSA, changed significantly with either the main effect of CO₂ or the main effect of warming, and varied by species and community (Table 2). *B. gracilis* root diameter increased with warming. In *P. smithii*, SRL increased by 88%, and SRSA increased by 50%, under the main effect of elevated CO₂ compared to ambient (Table 2). At the community level, root diameter decreased with elevated CO₂, whereas SRL and SRSA increased with elevated CO₂ (Table 2). Root morphology of *C. eleocharis* showed no statistical differences among field treatments ($P > 0.05$).

Table 1

Average *B. gracilis*, *C. eleocharis*, *P. smithii*, and community root C concentration, N concentration, and C:N ratio at 0–10 cm depth after seven years of elevated CO₂ and warming grouped into four field treatments; ct = ambient CO₂ and temperature, cT = ambient CO₂ and elevated temperature, Ct = elevated CO₂ and ambient temperature, and CT = elevated CO₂ and temperature. Values are means ± standard error, *P*-values are from two-way ANOVA, CO₂ by temperature. Values followed by the same letters did not differ by treatment based on least squares means separation with a Tukey–Kramer adjustment. Significant differences between treatments were determined at $\alpha = 0.05$.

Root ID	Field Tmt	Root C (%)	Root N (%)	Root C:N
<i>B. gracilis</i>	ct	37.1 (1.0) b	0.67 (0.02) a	56 (2)
	cT	37.2 (1.0) b	0.67 (0.01) a	55 (2)
	Ct	37.3 (0.3) b	0.61 (0.04) b	59 (3)
	CT	42.0 (2.0) a	0.60 (0.03) b	62 (3)
<i>C. eleocharis</i>	ct	39.5 (1.1)	0.75 (0.04)	54 (2) b
	cT	40.8 (0.9)	0.77 (0.04)	54 (2) b
	Ct	39.7 (2.2)	0.65 (0.02)	62 (2) a
	CT	42.5 (0.9)	0.73 (0.05)	55 (2) a
<i>P. smithii</i>	ct	27.4 (0.8) c	0.60 (0.04) b	52 (2)
	cT	33.6 (0.8) b	0.62 (0.02) b	55 (2)
	Ct	39.2 (1.4) a	0.70 (0.04) a	58 (3)
	CT	36.9 (1.8) ab	0.64 (0.03) a	61 (4)
community	ct	48.4 (0.6)	0.73 (0.01) b	67 (1) a
	cT	48.4 (0.2)	0.85 (0.03) a	57 (2) b
	Ct	48.0 (0.3)	0.71 (0.01) b	62 (4) a
	CT	47.6 (0.6)	0.79 (0.01) a	60 (2) b

ANOVA Table (Pr > F)

Root ID	2 FF CRD	Root C (%)	Root N (%)	Root C:N
<i>B. gracilis</i>	Block	0.17	0.91	0.089
	CO ₂	0.032	0.041	0.074
	Warming	0.034	1	0.72
	CO ₂ *Warming	0.043	1	0.51
<i>C. eleocharis</i>	Block	0.066	0.62	0.12
	CO ₂	0.48	0.1	0.027
	Warming	0.12	0.1	0.1
	CO ₂ *Warming	0.57	0.47	0.074
<i>P. smithii</i>	Block	0.44	0.35	0.1
	CO ₂	<0.0001	0.038	0.076
	Warming	0.15	0.38	0.28
	CO ₂ *Warming	0.0048	0.12	0.91
community	Block	0.61	0.68	0.99
	CO ₂	0.26	0.53	0.58
	Warming	0.74	0.018	0.036
	CO ₂ *Warming	0.68	0.65	0.16

3.4. Root carbon decomposition

Root decomposition rates fit the three-parameter decay model (Eq. (2)) well (Supplemental Fig. 1). Warming significantly increased the resistant root C decomposition rate, R_r , for *B. gracilis* roots by an average 24% compared to ambient temperature, and for *P. smithii* roots by an average 28% (Fig. 2). In contrast, community roots' R_r marginally significantly decreased by an average 12% with elevated CO₂ (Fig. 2). The other decay parameters, R_l and K_l , did not demonstrate significant climate change treatment effects.

3.5. Relationships between root chemistry, morphology and decomposition

Root morphology and decomposition rates were correlated with root C and N concentrations, but mainly when both species and the community were combined (Fig. 3). Root diameter was inversely correlated with %C and %N, while SRL was positively correlated (Fig. 3a–d). The decomposition rate of the resistant pool (R_r) was positively correlated with both %C and %N (Fig. 3e–f), and the decomposition rate of the labile pool (R_l) followed a similar pattern (data not shown). Interestingly, root decomposition parameters were not correlated with root C:N ratios. For individual species, %C

in *P. smithii* roots was inversely correlated with diameter ($P = 0.003$, $r = -0.64$) and positively with SRL ($P = 0.004$; $r = 0.65$). We found no significant linear relationships between root morphology and chemistry in *B. gracilis* or *C. eleocharis* ($P > 0.05$).

3.6. Root-induced priming of SOC

The $\delta^{13}\text{C}$ values of CO₂ respired from Soil and Soil + Roots varied over the course of the incubation, with a day by CO₂ treatment interaction (Fig. 4a and b). The differences in $\delta^{13}\text{C}$ values between the elevated and ambient CO₂ treatments were higher in the beginning of the experiment than after day 50, with and without roots. However, this treatment effect on the isotopic composition did not translate into a significant effect on priming. The average percent of SOC-derived CO₂ increased over the duration of the incubation from an average 41% on day three to an average 90% by day ninety-four. (Fig. 4c). Regardless of treatment, adding *P. smithii* roots to soil significantly reduced cumulative SOC decomposition by 10.7% at the end of the experiment (Fig. 4d).

4. Discussion

Following eight years of elevated CO₂ and seven years of warming we found unique belowground responses of plant species and the community to the climate change treatments, which suggests that plant community composition is a significant factor in maintaining high soil C stocks in this semiarid grassland with climate change (Mueller et al., 2016). Increased decomposition rates of roots exposed to warming treatments (Fig. 2), associated with their higher N concentrations (Table 1; Fig. 3), may contribute to formation of soil organic matter (Pendall et al., 2004). Moreover, a destructive harvest at the end of the PHACE experiment allowed us to demonstrate for the first time that crown biomass of two native species responded strongly to climate change. The increase of *C. eleocharis* crowns and roots with elevated CO₂, especially when combined with warming (Fig. 1), demonstrates a role for this subdominant C3 species – at the expense of the dominant C4, *B. gracilis* – in contributing to grassland community stability over eight years of exposure to future climate at the PHACE experiment (Zelikova et al., 2014). The negative priming by an important C3 grass, *P. smithii* (Fig. 4), provides evidence of plant-soil interactions in regulating ecosystem responses to climate change. This multi-component study thus provides mechanistic insights into the regulation of stable soil C pools by native grassland species exposed to climate change.

4.1. Crown and root biomass

Differences among species in belowground biomass responses to climate change appear to reflect intrinsic species adaptation strategies and alterations in soil resource availability under climate change. For example, the observed increase in *B. gracilis* crown biomass under warming independent of CO₂ may be a reflection of *B. gracilis*' resistance to drought (Weaver, 1968) and C4 photosynthetic pathway (Morgan et al., 2011), and is consistent with the expansion of its aboveground biomass with warming (Mueller et al., 2016). The positive effect of CO₂ on *C. eleocharis* root biomass and crown biomass (with warming only) could be due to both direct photosynthetic responses, which are common in C3 species, and the increase in N with the combination of CO₂ and warming, which might increase its ability to compete with more N-use efficient C4 grasses (Mueller et al., 2016). The increase in belowground growth in *C. eleocharis* under climate change parallels its aboveground expansion, and suggests that this species is an important contributor to the resilience of this grassland in response

Table 2

Average root morphology parameters (top table) and *P*-values (bottom table) by root type at 0–10 cm depth and following seven years of elevated CO₂ and warming grouped into four field treatments; ct = ambient CO₂ and temperature, cT = ambient CO₂ and elevated temperature, Ct = elevated CO₂ and ambient temperature, and CT = elevated CO₂ and temperature. RD = root diameter (mm), RTD = root tissue density (mg mm⁻³), SRL = specific root length (mm mg⁻¹), and SRSA = specific root surface area (mm² mg⁻¹). Top table values are means ± standard error in parentheses and bottom table values are *P*-values from two-way ANOVA, CO₂ by temperature. Values followed by the same letters did not differ by treatment based on least squares means separation with a Tukey-Kramer adjustment. Significant differences between treatments were determined at $\alpha = 0.05$.

Root ID	Field Treatment	RD (mm)	RTD (mg mm ⁻³)	SRL (mm mg ⁻¹)	SRSA (mm ² mg ⁻¹)
<i>B. gracilis</i>	ct	0.26 (0.01) b	0.554 (.039)	35 (3)	28 (2)
	cT	0.29 (0.01) a	0.523 (.030)	30 (3)	27 (2)
	Ct	0.26 (0.01) b	0.552 (.024)	34 (2)	28 (1)
	CT	0.28 (0.01) a	0.520 (.015)	32 (2)	28 (1)
<i>C. eleocharis</i>	ct	0.23 (0.02)	0.476 (.032)	56 (8)	39 (4)
	cT	0.22 (0.01)	0.466 (.013)	57 (6)	39 (2)
	Ct	0.24 (0.02)	0.520 (.019)	44 (6)	32 (3)
	CT	0.22 (0.01)	0.502 (.032)	56 (5)	37 (3)
<i>P. smithii</i>	ct	0.41 (0.04)	0.540 (.032)	16 (4) b	19 (3) b
	cT	0.41 (0.04)	0.472 (.021)	17 (3) b	21 (2) b
	Ct	0.35 (0.03)	0.467 (.047)	25 (5) a	26 (2) a
	CT	0.32 (0.05)	0.431 (.026)	35 (9) a	31 (4) a
community	ct	0.23 (0.004)a	0.495 (.015)	50 (3) b	36 (2) b
	cT	0.25 (0.02) a	0.475 (.022)	44 (4) b	34 (1) b
	Ct	0.22 (0.01) b	0.494 (.024)	55 (4) a	37 (2) a
	CT	0.20 (0.01) b	0.507 (.048)	65 (7) a	40 (3) a

ANOVA Table (Pr > F)					
Root ID	2 FF CRD	RD (mm)	RTD (mg mm ⁻³)	SRL (mm mg ⁻¹)	SRSA (mm ² mg ⁻¹)
<i>B. gracilis</i>	Block	0.5	0.14	0.62	0.3
	CO ₂	0.72	0.93	0.89	0.92
	Warming	0.039	0.27	0.16	0.62
	CO ₂ *Warming	0.58	0.98	0.58	0.7
	Block	0.011	0.7	0.056	0.15
<i>C. eleocharis</i>	CO ₂	0.62	0.15	0.26	0.2
	Warming	0.18	0.6	0.3	0.36
	CO ₂ *Warming	0.38	0.88	0.36	0.45
	Block	0.79	0.86	0.99	0.92
	CO ₂	0.055	0.15	0.029	0.015
<i>P. smithii</i>	Warming	0.66	0.19	0.37	0.28
	CO ₂ *Warming	0.66	0.67	0.45	0.62
	Block	0.42	0.23	0.15	0.06
	CO ₂	0.024	0.6	0.012	0.047
	Warming	0.79	0.91	0.63	0.67
community	CO ₂ *Warming	0.11	0.59	0.1	0.24

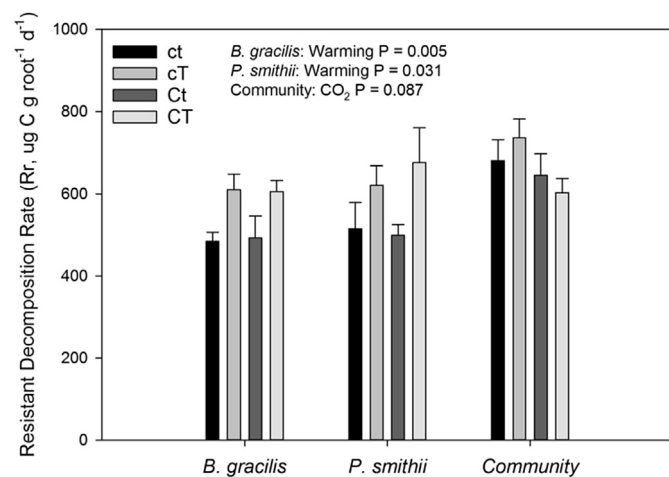


Fig. 2. Average resistant root C decomposition rate, *R_r*, from laboratory incubation of *B. gracilis*, *P. smithii*, and community roots collected from 0–10 cm depth following seven years of elevated CO₂ and warming grouped into four field treatments; ct = ambient CO₂ and temperature, cT = ambient CO₂ and elevated temperature, Ct = elevated CO₂ and ambient temperature, and CT = elevated CO₂ and temperature. Values are means ± standard error; *P*-values are from two-way ANOVA, CO₂ by temperature.

to climate change (Zelikova et al., 2014).

4.2. Root chemistry

Soil N availability may explain many of the changes in root chemistry in response to climate change, such as increased N immobilization by microorganisms and a decrease in root N with elevated CO₂, and increased N mineralization and root N under warming (Eissenstat et al., 2000; Gorissen and Cotrufo, 2000; Pendall et al., 2004; van Groenigen et al., 2005; de Graaff et al., 2006; Dijkstra et al., 2010; Pendall et al., 2011; Dieleman et al., 2012). Species-specific effects reflect different traits and strategies for nutrient acquisition. For instance, the increase in *P. smithii* root % C under elevated CO₂ at ambient temperature may be a consequence of greater C allocation to roots in response to declining soil N availability (Hunt et al., 1996). We speculate that the relatively low root C concentrations in this species may reflect a large amount of silica, because these elements can be inversely related in grass roots due to a trade-off in defense mechanisms (Frew et al., 2016). Root %N increased in *P. smithii* under elevated CO₂, possibly owing to access to soil N “hotspots” through construction of deeper or longer and thinner roots (Table 2) (Kemp and Williams, 1980; de Graaff et al., 2006; Dijkstra et al., 2008, 2010). Root %N decreased in *B. gracilis* under elevated CO₂, reflecting higher nutrient use

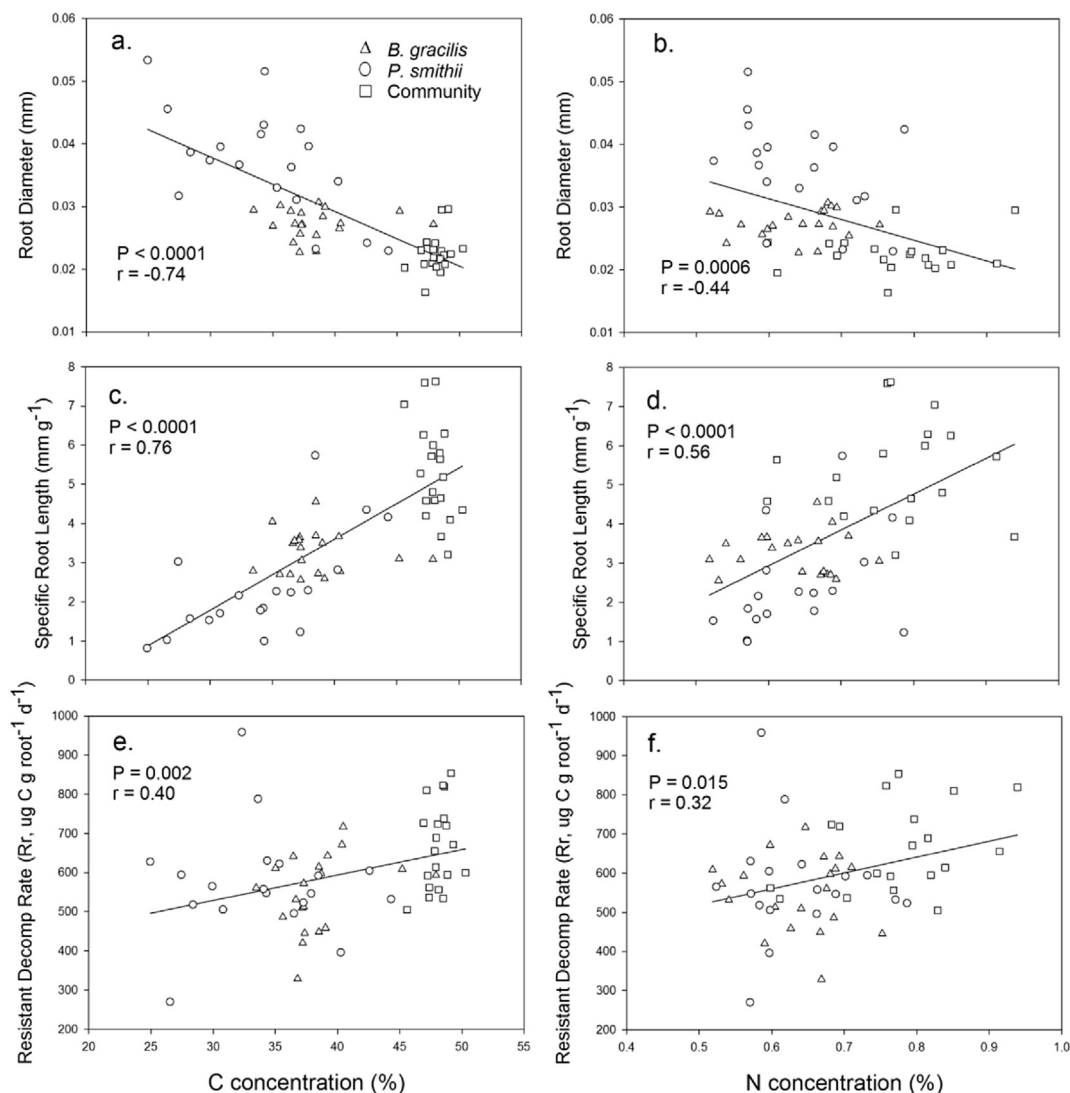


Fig. 3. Linear relationships between chemical and morphological properties for roots of *P. smithii*, *B. gracilis* and the community, collected at 0–10 cm depth following seven years of elevated CO₂ and warming. a) root C and root diameter (RD); b) root N and RD; c) root C and specific root length (SRL); d) root N and SRL; e) root C and resistant root decomposition rate; f) root N and resistant root decomposition rate. Treatments were, ct = ambient CO₂ and temperature, cT = ambient CO₂ and elevated temperature, Ct = elevated CO₂ and ambient temperature, and CT = elevated CO₂ and temperature. *P* and *r*²-values are from simple linear regression (*n* = 60).

efficiency by this C4 grass, and potentially increased competition with microbes.

Altered root C:N under elevated CO₂ and warming found in this study suggests potential changes in decomposability in the future (Birouste et al., 2012; Pendall et al., 2013). However, C:N ratios were not significant predictors of root decomposition in this study, possibly because C represents a range of compounds varying in degradability (van Groenigen et al., 2005; Freschet et al., 2012).

4.3. Root morphology

Root morphological responses to climate change may provide insight into soil resource availability, as roots are the main conduits for water and nutrients to the plant (Pendall et al., 2013). The increase in diameter of *B. gracilis* with warming may be due to a greater abundance of suberized than non-suberized roots in our samples from warmed plots (Suseela et al., 2017). A study monitoring *B. gracilis* root growth found non-suberized roots highly susceptible to turnover in dry soils, and that suberized roots have

greater root diameters than nonsuberized roots (Ares, 1976). Also, because suberin is a hydrophobic, resistant C compound that decreases water flow from roots into the soil, suberized roots may be favored in water-stressed soils (North, 1991; Meyer, 2013).

The linear relationships between root %C, diameter and SRL suggests that C can be allocated for the production of longer, thinner roots, two traits that favor nutrient acquisition (Prieto et al., 2015), and is consistent with our observations of higher root N concentrations in longer, thinner roots. Both SRL and SRSA increased in *P. smithii* roots under the main effect of elevated CO₂, possibly a consequence of soil water availability no longer constraining root exploration for soil sites with richer nutrient availability and faster N uptake (Reich and Cornelissen, 2014).

At the community-level we observed a decrease in diameter and increase in SRL and SRSA under the main effect of elevated CO₂, in agreement with a previous study (Carrillo et al., 2014). The production of longer and thinner roots under elevated CO₂ may be a similar response as suggested for *P. smithii*, where an increase in soil water content enables construction of longer and thinner roots,

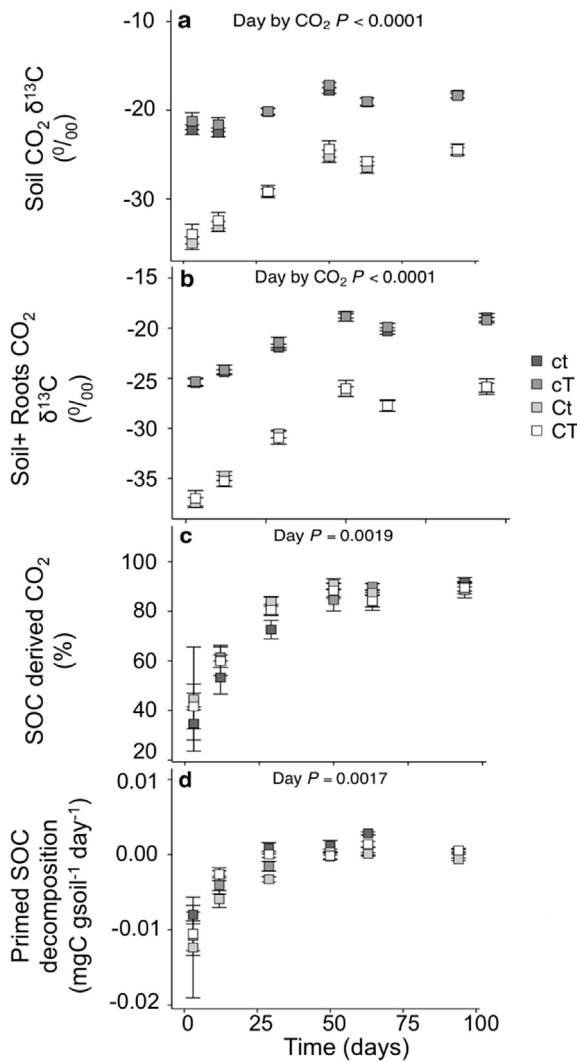


Fig. 4. Changes in $\delta^{13}\text{C}$ of CO_2 and priming of soil organic carbon (SOC) during the 94-day laboratory incubation decomposition. a) $\delta^{13}\text{C}$ of CO_2 generated from Soil; b) $\delta^{13}\text{C}$ of CO_2 generated from Soil + Roots; c) percentage of SOC-derived CO_2 ; and d) rate of SOC priming ($\text{mgC gsoil}^{-1} \text{day}^{-1}$). Soil was collected from 0–5 cm and *P. smithii* roots from 0–10 cm depth from four different field treatments applied for seven years; ambient CO_2 and temperature, ct, ambient CO_2 and warmed, cT, elevated CO_2 and ambient temperature, Ct, and combined elevated CO_2 and warmed, CT. Values are means \pm standard error and *P*-values are from three-way ANOVA, CO_2 by temperature by time (incubation day).

broadening the search for available N (Dijkstra et al., 2010; Reich and Cornelissen, 2014). Alternatively, the longer and thinner roots of the community may be driven by the increase in *C. eleocharis* root biomass under elevated CO_2 , as *C. eleocharis* has comparatively longer and thinner roots than either *B. gracilis* or *P. smithii* (Table 2). However, the overall different morphological responses between community-level and species-level roots to climate change suggest that an analysis of root traits at the community-level may mask species-level responses. Future studies in similar perennial grasslands would benefit from more comprehensive recovery and analysis of roots from all species present.

4.4. Root decomposition

In soils, resistant C pool dynamics strongly influence soil C sequestration (Reid et al., 2012), and transfer of root C to SOC pools

over the long term depends on their decomposability. An increase in C quality, and/or increased N concentrations, under warming in both *B. gracilis* and *P. smithii* may explain the increased decomposition rate responses of resistant root C (Silver and Miya, 2001). An increase in root C:N and a change in lignin concentration were thought to explain decreased decomposition of roots grown under elevated CO_2 following eight days of incubation (Gorissen et al., 1995). In contrast to our predictions, we found few relationships between root morphological parameters and decomposition rates, possibly because all roots were very fine in this semi-arid grassland.

4.5. SOC priming

The stimulation of negative SOC priming by the addition of *P. smithii* roots to the soil may be explained by greater availability of labile-C in *P. smithii* roots than in SOC causing a shift in microorganisms predominantly decomposing SOC to microorganisms mainly decomposing *P. smithii* roots (de Graaff et al., 2013). Since we found no significant change in root-induced negative priming of SOC among climate change treatments, short-term negative priming of SOC may persist to the same observed degree in the future, which may lead to SOC sequestration. However, extending our results to the field is complex because previous work at our site revealed that subdominant species increase in productivity, while dominant species (including *P. smithii*) decrease in productivity under climate change (Zelikova et al., 2014). Thus, a change in community composition may alter *P. smithii* root-induced priming effects. Also, we quantified priming during a three-month period under optimal lab conditions. Therefore, long-term storage of SOC due to root-induced priming may not occur in the field, where other factors, such as precipitation, temperature, competition, and microbial dynamics fluctuate.

Acknowledgments

We thank Y. Carrillo for insightful discussions; D. LeCain, L. Macdonald, M. Nie, S. Raut, D. Smith, S. Tamang, T.J. Zelikova and Y. Carrillo for their assistance in the field and lab; and C. Macdonald and D. Wolfe at the Stable Isotope Facility at the University of Wyoming for help with sampling and analysis. Research for this project was funded by the U.S. Department of Agriculture, the USDA-CSREES Soil Processes Program (#2008-35107-18655), the U.S. Department of Energy Office of Science (BER) through the Terrestrial Ecosystem Science program (#DE-SC0006973), the Western Regional Center of the National Institute for Climatic Change Research, and the National Science Foundation (DEB#1021559).

Appendix A. Supplementary data

Supplementary data related to this article can be found at <http://dx.doi.org/10.1016/j.soilbio.2017.08.022>.

References

- Allard, V., Newton, P.C.D., Lieffering, M., Soussana, J.F., Carran, R.A., Matthew, C., 2005. Increased quantity and quality of coarse soil organic matter fraction at elevated CO_2 in a grazed grassland are a consequence of enhanced root growth rate and turnover. *Plant and Soil* 276, 49–60.
- Ares, J., 1976. Dynamics of the root system of blue grama. *Journal of Range Management* 29, 208–213.
- Bardgett, R.D., Mommer, L., De Vries, F.T., 2014. Going underground: root traits as drivers of ecosystem processes. *Trends in Ecology & Evolution* 29, 692–699.
- Birouste, M., Kazakou, E., Blanchard, A., Roumet, C., 2012. Plant traits and decomposition: are the relationships for roots comparable to those for leaves? *Annals of Botany* 109, 463–472.
- Burke, I.C., Bontti, E.E., Barrett, J.E., Lowe, P.N., Lauenroth, W.K., Riggle, R., 2013. Impact of labile and recalcitrant carbon treatments on available nitrogen and

- plant communities in a semiarid ecosystem. *Ecological Applications* 23, 537–545.
- Carrillo, Y., Dijkstra, F.A., LeCain, D., Morgan, J.A., Blumenthal, D., Waldron, S., Pendall, E., 2014. Disentangling root responses to climate change in a semiarid grassland. *Oecologia* 175, 699–711.
- Carrillo, Y., Pendall, E., Dijkstra, F.A., Morgan, J.A., Newcomb, J.M., 2011. Response of soil organic matter pools to elevated CO₂ and warming in a semi-arid grassland. *Plant and Soil* 347, 339–350.
- Carrillo, Y., Dijkstra, F.A., Pendall, E., Morgan, J.A., Blumenthal, D.M., 2012. Controls over soil nitrogen pools in a semiarid grassland under elevated CO₂ and warming. *Ecosystems* 15, 761–774.
- Craine, J.M., Wedin, D.A., Chapin, F.S.I., Reich, P.B., 2003. The dependence of root system properties on root system biomass of 10 North American grassland species. *Plant and Soil* 250, 39–47.
- de Graaff, M.-A., Schadt, C.W., Rula, K., Six, J., Schweitzer, J.A., Classen, A.T., 2011. Elevated CO₂ and plant species diversity interact to slow root decomposition. *Soil Biology and Biochemistry* 43, 2347–2354.
- de Graaff, M.-A., van Groenigen, K.-J., Six, J., Hungate, B., van Kessel, C., 2006. Interactions between plant growth and soil nutrient cycling under elevated CO₂: a meta-analysis. *Global Change Biology* 12, 2077–2091.
- de Graaff, M.A., Six, J., Jastrow, J.D., Schadt, C.W., Wullschlegel, S.D., 2013. Variation in root architecture among switchgrass cultivars impacts root decomposition rates. *Soil Biology & Biochemistry* 58, 198–206.
- Dieleman, W.I., Vicca, S., Dijkstra, F.A., Hagedorn, F., Hovenden, M.J., Larsen, K.S., Morgan, J.A., Volder, A., Beier, C., Dukes, J.S., King, J., Leuzinger, S., Linder, S., Luo, Y., Oren, R., De Angelis, P., Tingey, D., Hoosbeek, M.R., Janssens, I.A., 2012. Simple additive effects are rare: a quantitative review of plant biomass and soil process responses to combined manipulations of CO₂ and temperature. *Global Change Biology* 18, 2681–2693.
- Dijkstra, F.A., Blumenthal, D., Morgan, J.A., 2010. Contrasting effects of elevated CO₂ and warming on nitrogen cycling in a semiarid grassland. *New Phytologist* 187, 426–437.
- Dijkstra, F.A., Pendall, E., Mosier, A.R., King, J.Y., Milchunas, D.G., Morgan, J.A., 2008. Long-term enhancement of N availability and plant growth under elevated CO₂ in a semi-arid grassland. *Functional Ecology* 22, 975–982.
- Eissenstat, D.M., Wells, C.E., Yanai, R.D., Whitbeck, J.L., 2000. Building roots in a changing environment: implications for root longevity. *New Phytologist* 147, 33–42.
- Freschet, G.T., Aerts, R., Cornelissen, J.H.C., 2012. A plant economics spectrum of litter decomposability. *Functional Ecology* 26, 56–65.
- Frew, A., Powell, J.R., Sallam, N., Allsopp, P.G., Johnson, S.N., 2016. Trade-offs between silicon and phenolic defences may explain enhanced performance of root herbivores on phenolic-rich plants. *Journal of Chemical Ecology* 42, 768–771.
- Gorissen, A., Cotrufo, M.F., 2000. Decomposition of leaf and root tissue of three perennial grass species grown at two levels of atmospheric CO₂ and N supply. *Plant and Soil* 224, 75–84.
- Gorissen, A., van Ginkel, J.H., Keurentjes, J.J.B., Van Veen, J.A., 1995. Grass root decomposition is retarded when by Gorissen.pdf. *Soil Biology & Biochemistry* 27, 117–120.
- Heinemeyer, A., Tortorella, D., Petrovičová, B., Gelsomino, A., 2012. Partitioning of soil CO₂ flux components in a temperate grassland ecosystem. *European Journal of Soil Science* 63, 249–260.
- Hui, D., Jackson, R.B., 2006. Geographical and interannual variability in biomass partitioning in grassland ecosystems: a synthesis of field data. *New Phytologist* 169, 85–93.
- Hunt, H.W., Elliott, E.T., Detling, J.K., Morgan, J.A., Chen, D.X., 1996. Responses of a C3 and a C4 perennial grass to elevated CO₂ and temperature under different water regimes. *Global Change Biology* 2, 35–47.
- Jackson, R.B., Mooney, H.A., Schulze, E.-D., 1997. A global budget for fine root biomass, surface area, and nutrient contents. *Proceedings of the National Academy of Sciences of the United States of America* 94, 7362–7366.
- Jones, M.B., Donnelly, A., 2004. Carbon sequestration in temperate grassland ecosystems and the influence of management, climate and elevated CO₂. *New Phytologist* 164, 423–439.
- Kemp, P.R., Williams, G.J., 1980. A physiological basis for niche separation between *Agropyron smithii* (C³) and *Bouteloua gracilis* (C⁴). *Ecology* 61, 846–858.
- Kuzyakov, Y., Friedel, J.K., Stahr, K., 2000. Review of mechanisms and quantification of priming effects. *Soil Biology & Biochemistry* 32, 1485–1498.
- LeCain, D., Smith, D., Morgan, J., Kimball, B.A., Pendall, E., Miglietta, F., 2015. Microclimatic performance of a free-air warming and CO₂ enrichment experiment in windy Wyoming, USA. *PLoS One* 10, e0116834.
- LeCain, D.R., Morgan, J.A., Milchunas, D.G., Mosier, A.R., Nelson, J.A., Smith, D.P., 2006. Root biomass of individual species, and root size characteristics after five years of CO₂ enrichment on native shortgrass steppe. *Plant and Soil* 279, 219–228.
- Mary, B., Mariotti, A., Morel, J.L., 1992. Use of ¹³C variations at natural abundance for studying the biodegradation of root mucilage, roots and glucose in soil. *Soil Biology and Biochemistry* 24, 1065–1072.
- Meyer, C.J.A.P., C.A., 2013. Structure and function of three suberized cell layers: Epidermis, Exodermis, and Endodermis. In: Eshel, A.A.B., T. (Ed.), *Plant Roots: the Hidden Half*, fourth ed. Taylor and Francis Group, Boca Raton, FL, 5–15–20.
- Milchunas, D.G., Lauenroth, W.K., 2001. Belowground primary production by carbon isotope decay and long-term root biomass dynamics. *Ecosystems* 4, 139–150.
- Mokany, K., Raison, R.J., Prokushkin, A.S., 2006. Critical analysis of root : shoot ratios in terrestrial biomes. *Global Change Biology* 12, 84–96.
- Morgan, J.A., LeCain, D.R., Pendall, E., Blumenthal, D.M., Kimball, B.A., Carrillo, Y., Williams, D.G., Heisler-White, J., Dijkstra, F.A., West, M., 2011. C₄ grasses prosper as carbon dioxide eliminates desiccation in warmed semi-arid grassland. *Nature* 476, 202–205.
- Mueller, K.E., Blumenthal, D.M., Pendall, E., Carrillo, Y., Dijkstra, F.A., Williams, D.G., Follett, R.F., Morgan, J.A., 2016. Impacts of warming and elevated CO₂ on a semi-arid grassland are non-additive, shift with precipitation, and reverse over time. *Ecology Letters* 19, 956–966.
- Nie, M., Pendall, E., Bell, C., Gasch, C.K., 2013. Positive climate feedbacks of soil microbial communities in a semi-arid grassland. *Ecology Letters* 16, 234–241.
- North, G.B.a.N.P.S., 1991. Changes in hydraulic conductivity and anatomy caused by drying and rewetting roots of agave deserti (Agavaceae). *American Journal of Botany* 78, 906–915.
- Nowak, R.S., Ellsworth, D.S., Smith, S.D., 2004. Functional responses of plants to elevated atmospheric CO₂ - do photosynthetic and productivity data from FACE experiments support early predictions? *New Phytologist* 162, 253–280.
- Pendall, E., Bridgman, S., Hanson, P.J., Hungate, B., Kicklighter, D.W., Johnson, D.W., Law, B.E., Luo, Y., Megonigal, J.P., Olsrud, M., Ryan, M.G., Wan, S., 2004. Below-ground process responses to elevated CO₂ and temperature: a discussion of observations, measurement methods, and models. *New Phytologist* 162, 311–322.
- Pendall, E., Heisler-White, J.L., Williams, D.G., Dijkstra, F.A., Carrillo, Y., Morgan, J.A., LeCain, D.R., 2013. Warming reduces carbon losses from grassland exposed to elevated atmospheric carbon dioxide. *PLoS One* 8.
- Pendall, E., King, Y.J., 2007. Soil organic matter dynamics in grassland soils under elevated CO₂: insights from long-term incubations and stable isotopes. *Soil Biology & Biochemistry* 39, 2628–2639.
- Pendall, E., Osanai, Y.U.L., Williams, A.L., Hovenden, M.J., 2011. Soil carbon storage under simulated climate change is mediated by plant functional type. *Global Change Biology* 17, 505–514.
- Pilon, R., Picon-Cochard, C., Bloor, J.M.G., Revaillet, S., Kuhn, E., Falcimagne, R., Balandier, P., Soussana, J.F., 2013. Grassland root demography responses to multiple climate change drivers depend on root morphology. *Plant and Soil* 364, 395–408.
- Prieto, I., Roumet, C., Cardinael, R., Dupraz, C., Jourdan, C., Kim, J.H., Maeght, J.L., Mao, Z., Pierret, A., Portillo, N., Roupard, O., Thammahacksa, C., Stokes, A., Cahill, J., 2015. Root functional parameters along a land-use gradient: evidence of a community-level economics spectrum. *Journal of Ecology* 103, 361–373.
- Reich, P.B., Cornelissen, H., 2014. The world-wide 'fast-slow' plant economics spectrum: a traits manifesto. *Journal of Ecology* 102, 275–301.
- Reid, J.P., Adair, E.C., Hobbie, S.E., Reich, P.B., 2012. Biodiversity, nitrogen deposition, and CO₂ affect grassland soil carbon cycling but not storage. *Ecosystems* 15, 580–590.
- Silver, W.L., Miya, R.K., 2001. Global patterns in root decomposition: comparisons of climate and litter quality effects. *Oecologia* 129, 407–419.
- Smith, S.W., Woodin, S.J., Pakeman, R.J., Johnson, D., van der Wal, R., 2014. Root traits predict decomposition across a landscape-scale grazing experiment. *New Phytologist* 203, 851–862.
- Suseela, V., Tharayil, N., Pendall, E., Rao, A., 2017. Warming and elevated CO₂ alter the suberin chemistry in roots of photosynthetically divergent grass species. *Annals of Botany in Revision*.
- van Groenigen, K.-J., Gorissen, A., Six, J., Harris, D., Kuikman, P.J., van Groenigen, J.W., van Kessel, C., 2005. Decomposition of ¹⁴C-labeled roots in a pasture soil exposed to 10 years of elevated CO₂. *Soil Biology and Biochemistry* 37, 497–506.
- Vivanco, L., Austin, A.T., 2006. Intrinsic effects of species on leaf litter and root decomposition: a comparison of temperate grasses from North and South America. *Oecologia* 150, 97–107.
- Weaver, J.E., 1968. *Prairie Plants and Their Environment: a Fifty-year Study in the Midwest*. University of Nebraska Press, Lincoln, NE.
- White, S.R., Carlyle, C.N., Fraser, L.H., Cahill Jr., J.F., 2012. Climate change experiments in temperate grasslands: synthesis and future directions. *Biology Letters* 8, 484–487.
- Zelikova, T.J., Blumenthal, D.M., Williams, D.G., Souza, L., LeCain, D.R., Morgan, J., Pendall, E., 2014. Long-term exposure to elevated CO₂ enhances plant community stability by suppressing dominant plant species in a mixed-grass prairie. *PNAS*. <http://dx.doi.org/10.1073/pnas.1414659111>.